

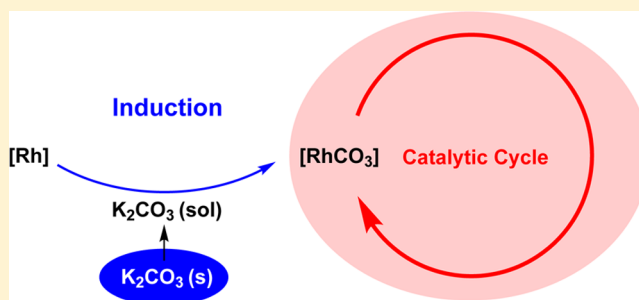
Investigations into the Kinetic Modeling of the Direct Alkylation of Benzylic Amines: Dissolution of K_2CO_3 Is Responsible for the Observation of an Induction Period

Robert Pollice and Michael Schnürch*

Institute of Applied Synthetic Chemistry, Vienna University of Technology, Getreidemarkt 9/163-OC, Vienna 1060, Austria

S Supporting Information

ABSTRACT: Investigations into the kinetics of a Rh(I)-catalyzed direct C–H alkylation of benzylic amines with alkenes revealed that K_2CO_3 , which is effectively insoluble in the reaction mixture, is only needed in the beginning of the reaction. During the concomitant induction period, K_2CO_3 is proposed to dissolve to a vanishingly small extent and the Rh-precatalyst irreversibly reacts with dissolved K_2CO_3 to form the active catalyst. The duration of this induction period is dependent on the molar loading, the specific surface, the H_2O content of K_2CO_3 , and agitation, and these dependences can be rationalized based on a detailed kinetic model.



1. INTRODUCTION

Transition metal-catalyzed C–H activation reactions have experienced tremendous advances in recent years.¹ As a result of these advances, direct functionalization of sp^2 -hybridized carbon centers is well established in the field,² and an increasing number of protocols for the coupling of $C(sp^3)$ –H bonds is emerging.³ In many of these metal-catalyzed direct C–H functionalizations, heterogeneous bases are used as reactants⁴ and in some cases also as cocatalysts.⁵ Especially, carbonates are widely used in the field.⁶ However, detailed studies with respect to the influence of the heterogeneous base employed in the reaction are usually avoided. In fact, to the best of our knowledge, there has not been any literature report investigating the common main influence parameters associated with heterogeneous reactions in detail in the field of C–H activation reactions. One reason may be that the heterogeneous nature of the corresponding reaction mixtures makes these studies more challenging. Our group recently reported a Ru(II)-catalyzed arylation of benzylic amines with aryl halides using K_2CO_3 as reactant,⁷ and a Rh(I)-catalyzed alkylation of benzylic amines with either alkyl bromides or alkenes using K_2CO_3 as reactant and cocatalyst, respectively.⁸ In the latter publication we reported (inter alia) a significant dependence of the initial reaction rate on the H_2O content of the K_2CO_3 batch used, which was, to the best of our knowledge, the first literature-reported dependence of this kind in metal-catalyzed coupling reactions. However, there were several unresolved questions, namely the role of K_2CO_3 in the reaction and the reason why H_2O would significantly speed the reaction. On the basis of these open ends, we decided to further investigate this transformation both mechanistically and kinetically, focusing on the role of K_2CO_3 and its influence on the reaction rate. We used this reaction as a benchmark to gain insight into the main

influence factors associated with heterogeneous bases in metal-catalyzed reactions and to elucidate one of the associated underlying reaction mechanisms.

2. RESULTS AND DISCUSSION

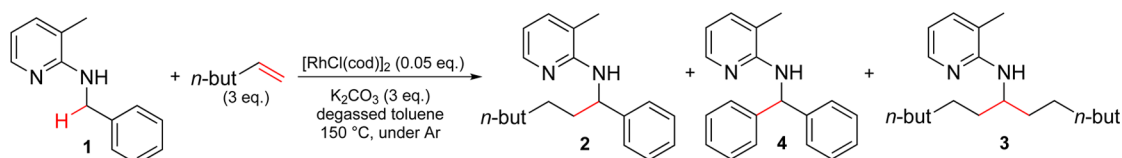
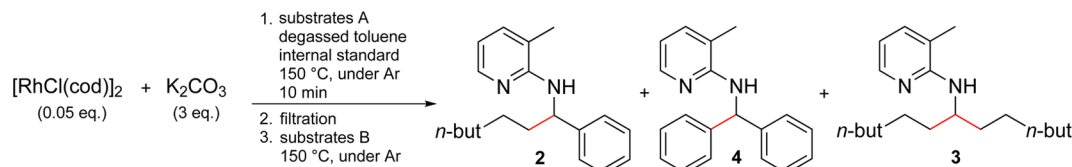
2.1. Preliminary Observations. Because we did not observe an induction period under the optimized reaction conditions in the direct alkylation of benzylic amines (cf. Scheme 1)⁸ we performed initial rate experiments to determine the partial reaction orders with respect to all starting materials (details in the Supporting Information). In light of our later observations (vide infra) it is important that not observing an induction period does not mean that there is none.⁹

First-order dependences with respect to **1** and $[RhCl(cod)]_2$ and a zero-order dependence with respect to hex-1-ene were observed. Interestingly, we also observed a first-order dependence on the initial molar loading of K_2CO_3 , which is almost insoluble in the reaction mixture, when decreasing its amount compared to the optimized reaction conditions. This prompted us to focus on experiments investigating the role of K_2CO_3 in the reaction. Conceptually, K_2CO_3 is not required as a stoichiometric base because there is no formation of acid as byproduct in this reaction.

2.2. Induction Studies. To further examine the role of K_2CO_3 , the following experiments were designed. In the first experiment (cf. Table 1) all starting materials of the direct alkylation were reacted for 10 min. Afterward, the reaction was stopped and filtered. The solid residue was reacted with **1** and hex-1-ene again, and the filtrate was reacted as obtained after

Received: June 12, 2015

Published: July 28, 2015

Scheme 1. Reaction Scheme for the Direct C–H Alkylation of **1** Using Hex-1-eneTable 1. Induction Studies of the Direct Alkylation of Benzylic Amines Using Alkenes^a

entry	substrates A	substrates B	rate ^b [10 ⁻⁵ mol·L ⁻¹ ·s ⁻¹]
1	1 (1 equiv) hex-1-ene (3 equiv)	–	5.7 ± 0.4
2	–	1 (1 equiv) hex-1-ene (3 equiv)	5.2 ± 0.3
3	1 (1 equiv)	hex-1-ene (3 equiv)	5.2 ± 0.1
4	hex-1-ene (3 equiv)	1 (1 equiv)	5.4 ± 0.2

^aDodecane was used as internal standard. ^bAfter filtration of the reaction mixture during 6.61 min. Errors are determined over three GC measurements.

the filtration. In the filtrate, the reaction continued with unaffected reaction rate; the solid residue, however, did not show any considerable catalytic activity. On the basis of this result, additional experiments were performed heating $[\text{RhCl}(\text{cod})]_2$ and K_2CO_3 together with no additional starting material, with **1** and with hex-1-ene, respectively, in the first 10 min before filtration and adding all the remaining substrates after filtration before continuing the reaction. The corresponding results are shown in Table 1.

These results implicate that K_2CO_3 is only needed in the beginning of the reaction, and this suggests that there is an induction period in which K_2CO_3 reacts with $[\text{RhCl}(\text{cod})]_2$ to form the catalytically active species for the direct alkylation of **1**. The observed first-order dependence of the initial reaction rate on the initial molar loading of K_2CO_3 is simply a result of the presence of an observable induction period under these reaction conditions which was evident from the determination of the kinetic time course with a significantly reduced initial molar loading of K_2CO_3 (details in the Supporting Information). On the basis of these results, it can be concluded that the actual catalysis is homogeneous and K_2CO_3 acts as a cocatalyst, and after the induction period, the residual solid has no further role in the catalytic reaction.

We also wanted to know whether it was possible to isolate a definite Rh-complex from the reaction of $[\text{RhCl}(\text{cod})]_2$ and K_2CO_3 in toluene so we reacted them for 10 min at 150 °C as before and removed excess K_2CO_3 by filtration and all the volatiles in vacuo. The obtained solid was analyzed by ATR-IR which showed a sharp band at 1572.6 cm^{-1} . This is indicative of a carbonyl group originating from a carbonato complex.¹⁰ The full ATR-IR spectrum is given in the Supporting Information. Attempts to obtain single crystals suitable for X-ray crystallography were unsuccessful. ¹H NMR did not show any significant peaks. When we used the obtained solid instead of the precatalyst $[\text{RhCl}(\text{cod})]_2$ and K_2CO_3 under the usual reaction conditions, catalytic activity was observed but the reaction proceeded significantly slower compared to the

optimized reaction conditions.¹¹ While this shows that a catalytically active species can be isolated from the reaction of $[\text{RhCl}(\text{cod})]_2$ and K_2CO_3 in toluene, it also suggests that under the optimized reaction conditions a different catalytically active species is present.

2.3. Kinetic Modeling of the Induction. After having established that K_2CO_3 is only needed in an induction period, we were interested in the kinetic modeling of this induction, which is a heterogeneous reaction. To gather more information about it, the common influence parameters of heterogeneous reactions were investigated. Therefore, we measured the particle size distributions and BET specific surface areas of several different K_2CO_3 batches and also determined the corresponding initial reaction rates in the direct alkylation of **1**. It could be shown that K_2CO_3 batches with higher specific surface areas indeed show a faster reaction (cf. Figure 1).

Additionally, agitation also accelerates the induction. Furthermore, H_2O contained in K_2CO_3 was also shown to significantly speed this reaction.⁸ More details about these and additional experiments and also about the consideration of alternative kinetic models for the induction are found in the Supporting Information. On the basis of these results, the following kinetic model for the induction is proposed. Solid K_2CO_3 dissolves to a vanishingly low extent in the reaction mixture and dissolved K_2CO_3 immediately reacts with a Rh-species to form a Rh-carbonato species, which is proposed to be the catalytically active species in the direct C–H alkylation of **1**. We propose the catalytically active species to be a carbonato species because we could obtain a carbonato species from the reaction of $[\text{RhCl}(\text{cod})]_2$ with K_2CO_3 in toluene (vide supra). However, we cannot fully exclude that the catalytically active species under the optimized reaction conditions actually is a hydroxido complex formed from deprotonation of H_2O introduced with K_2CO_3 .

Induction model-rate-determining dissolution of K_2CO_3 :

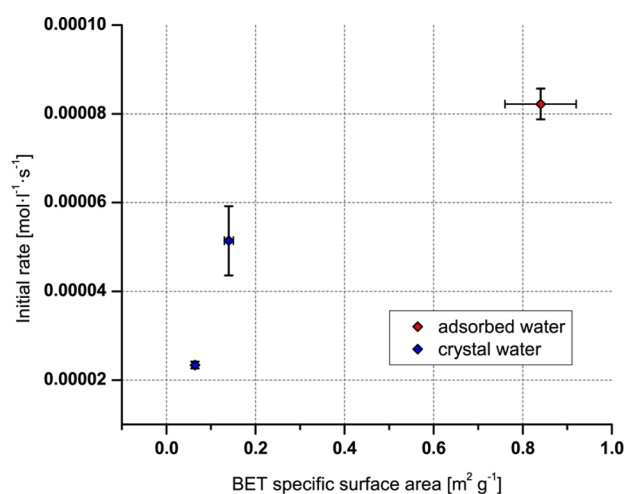
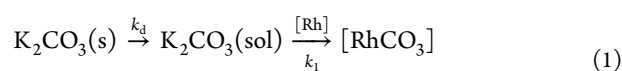


Figure 1. Dependence of the initial rate on the BET specific surface of K_2CO_3 containing about 15–16 mass % H_2O in the direct C–H alkylation of **1** using hex-1-ene.



On the basis of this model, the concentration time profile of $[RhCO_3]$ during the induction period can be described with eq 2. The corresponding mathematical derivation is found in the Supporting Information. Solubilization of K_2CO_3 is assumed to be slow compared to consecutive reaction with a Rh-species present in solution to form the active catalyst.

$$c([RhCO_3])(t) = \frac{DMS}{\delta} c_s c_0(K_2CO_3)t \quad (2)$$

where t is the time during the induction period [s], D is the diffusion coefficient of K_2CO_3 dissolved in toluene [$m^2 s^{-1}$], δ is the thin static solvent layer (solvent adheres tightly to the surface) [m], c_s is the saturation concentration of K_2CO_3 in solution [$mol \cdot m^{-3}$], M is the molar mass of K_2CO_3 [$kg mol^{-1}$],

S is the specific surface of K_2CO_3 [$m^2 \cdot kg^{-1}$], and $c_0(K_2CO_3)$ is the initial molar loading of K_2CO_3 in the reaction [$mol \cdot m^{-3}$].

The concentration of $[RhCO_3]$ increases linearly until all of the initial catalyst precursor $[RhCl(cod)_2]$ is converted.¹² This kinetic model can qualitatively explain the observed first-order dependence on the initial molar loading of K_2CO_3 when going to lower initial K_2CO_3 amounts. It can also explain why H_2O contained in K_2CO_3 would increase the initial reaction rate. The H_2O will be partially dissolved into the reaction mixture, resulting in a higher solubility of K_2CO_3 and therefore in an increased saturation concentration c_s of K_2CO_3 which directly leads to an increased reaction rate of the induction. Furthermore, the dependence on the specific surface of K_2CO_3 is directly evident from eq 2. Additionally, the dependence of the initial reaction rate on stirring can also be easily explained because no stirring would result in an increase of the thickness of the static solvent layer δ resulting in a prolonged induction.

Such kinetic behavior of heterogeneous solids, which are widely used in the field of metal-catalyzed coupling reactions, has, to the best of our knowledge, not been reported in the literature for related transformations. A similar kinetic description of solubilization of one reactant has been reported in solid–liquid phase transfer catalysis.¹³ In addition, studies on the influence of specific surface area and H_2O content of a heterogeneous base in C–H activation reactions have not been reported either. Thus, these results will be of significant interest for future research in this field because in many examples of metal-catalyzed direct functionalizations heterogeneous bases or other reagents are used. It would be surprising if this transformation were unique in showing such a significant dependence on the above-mentioned parameters. We believe that the kinetic description established in this work is applicable to reactions requiring stoichiometric amounts of heterogeneous base as well. These results obtained raise for example the question whether differences in screening results with different bases (e.g., alkali metal carbonates) really stem from the influence of the different counterions or are rather an effect of

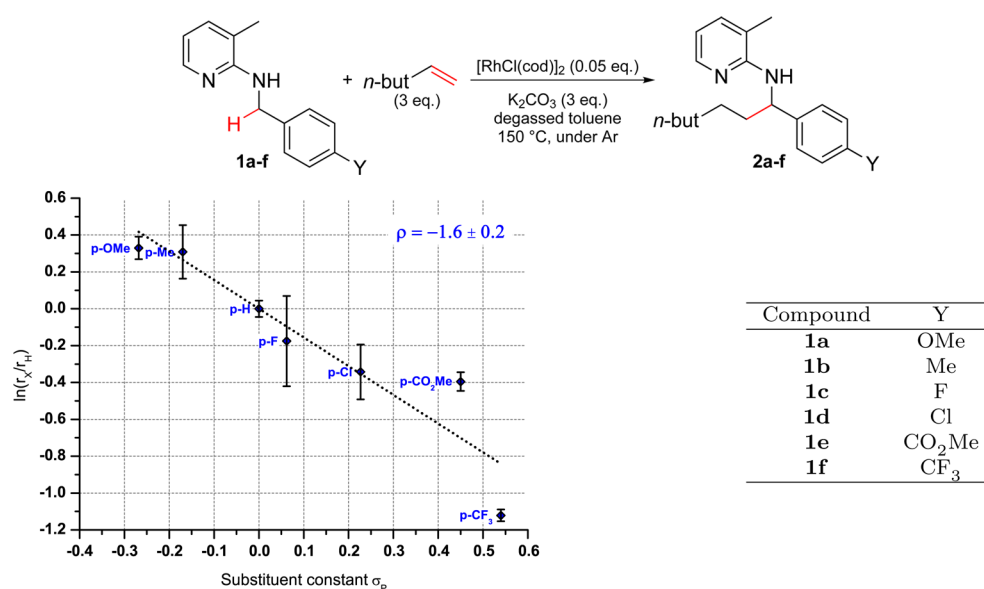


Figure 2. Determination of the electronic influence of substituents on the benzyl group of benzylic amines on the reaction rate in the direct C–H alkylation of **1** using hex-1-ene.

adsorbed H₂O and specific surface area. Therefore, these parameters have to be considered in future studies when such reactions are optimized and are potential targets for finetuning reaction conditions.

2.4. Electronic Influence on Benzylic Amines. Another aspect of interest was the electronic influence of benzylic amines on the reaction. Therefore, a Hammett plot¹⁴ was constructed from the initial rates of several benzylic amines **1a–f** (cf. Figure 2).¹⁵

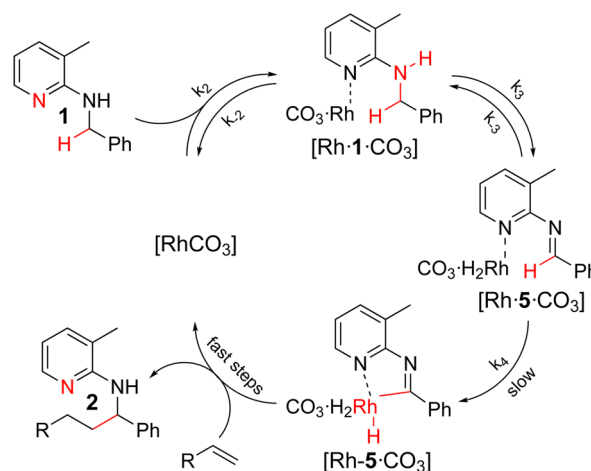
The reaction constant of -1.6 ± 0.2 indicates that the rate is accelerated by electron-donating groups on the benzylic amine. This result is discussed later on the basis of the proposed kinetic model.

2.5. Temperature Dependence of the Initial Rate. We were also interested to determine the temperature dependence of the reaction rate after the induction period and hence the activation parameters of the catalytic cycle. To investigate the temperature dependence of the reaction rate, the initial reaction rates were determined at five different temperatures. To accurately determine the initial reaction rates, five data points at different reaction times at every temperature were determined. The corresponding initial rates were obtained from linear regressions through these data points (details in the Supporting Information). From these initial reaction rates at different temperatures the activation parameters were calculated on the basis of the Eyring equation.¹⁶ The enthalpy of activation ΔH^\ddagger was found to be (148.8 ± 0.7) kJ mol⁻¹ or (35.6 ± 0.2) kcal·mol⁻¹ and the entropy of activation ΔS^\ddagger to be (81.4 ± 1.4) J mol⁻¹·K⁻¹ or (19.5 ± 0.3) eu based on the derived rate law for the reaction (vide infra). The enthalpy of activation shows a quite high value explaining the big temperature dependence of the reaction rate, and the entropy of activation shows a significant positive value showing that a significant degree of disorder is generated prior to or in the turnover-limiting step.

2.6. Kinetic Modeling of the Catalytic Cycle. On the basis of all the experimental results for the direct alkylation using alkenes, the following kinetic model for the catalytic cycle is proposed (cf. Scheme 2). This only shows the simplified kinetic model and not the complete catalytic cycle. A more complete catalytic cycle was proposed previously by us.⁸

This reaction has been proposed by us to occur via imine intermediates.⁸ We remain very vague with respect to the ligands on Rh because almost nothing is known about them so far. In the first step, **1** coordinates to [RhCO₃], which is proposed to be the resting state, to form [Rh·**1**·CO₃]. This coordination is followed by reversible interconversion to the corresponding complex [Rh·**5**·CO₃] of imine **5**. The turnover-limiting step is suggested to be oxidative addition into the C(sp²)–H bond of the imine complex. In the following steps of the catalytic cycle, which are proposed to be fast compared to the previous steps, hex-1-ene inserts into the Rh–H bond to form a Rh–alkyl complex which then reductively eliminates to form the alkylated imine. The imine is interconverted to the alkylated amine **2** which is released as the reaction product and regenerates [RhCO₃]. The general course of the proposed catalytic cycle has been discussed in more detail previously.⁸ It should be noted that the formation of **2** is assumed to be effectively irreversible in this kinetic model. This is only true in an initial reaction period because its formation was shown to be actually reversible.⁸ Furthermore, in the proposed kinetic model all Rh-species are assumed to be monomeric. However, on the basis of the experimental results at hand, this cannot be

Scheme 2. Proposed Simplified Kinetic Model for the Direct C–H Alkylation of Benzylic Amines Using Alkenes^a



^aEquations are not balanced with respect to total charge for clarity. It is unclear yet how H₂ is associated to the Rh-catalyst.

determined and the catalytic cycle may as well proceed over dimeric Rh-species as is the catalyst precursor [RhCl(cod)]₂.

At least in an initial reaction period, the reaction follows the following rate law.

$$r = k_4 K_3 K_2 c([\text{RhCO}_3]) c_0(\mathbf{1}) \quad (3)$$

Now the observed kinetic isotope effects (KIE), previously reported by us (cf. Figure 3),⁸ reaction constant, and activation

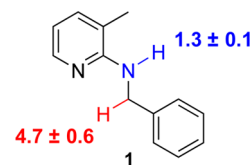


Figure 3. KIEs previously determined by us⁸ with respect to the benzylic C–H bond and the N–H bond in the direct alkylation of benzylic amines using hex-1-ene.

parameters can be interpreted on the basis of the proposed kinetic model. The KIEs were determined from the observed initial reaction rates of independent experiments using either deuterated or undeuterated substrate.

The large primary KIE of about 4–5 with respect to the benzylic C–H bond is mainly explained by the oxidative addition into the C–H bond of the imine as the turnover-limiting step. However, there may also be an equilibrium isotope effect (EIE) influencing K_3 because the interconversion of amine to imine also involves breaking one of the benzylic C–H bonds. This EIE, however, is not expected to be dominant. The large value supports the proposal that oxidative addition into the C–H bond is turnover-limiting both when the undeuterated and when the deuterated substrate is employed. Furthermore, this also supports our proposal that all steps in the catalytic cycle following oxidative addition into the C–H bond are fast compared to the slowest step. The observed small KIE of 1.3 with respect to the N–H bond of the amine is also suggested to originate from an EIE influencing K_3 because the corresponding N–H bond is broken in this step as well. The reaction constant of -1.6 with respect to functional groups on the benzylic amine supports turnover-limiting oxidative

addition into the C–H bond. However, earlier steps might also have a significant influence on the reaction constant. The large enthalpy of activation suggests that high energy transition states are involved in the catalytic cycle. The largely positive entropy of activation suggests that a significant degree of disorder is created in the course of the catalytic cycle until the turnover-limiting step, but not much is known of the exact nature of the corresponding elementary steps and the involved intermediates so an interpretation is omitted here.

3. CONCLUSION

The role of K_2CO_3 in the direct C–H alkylation of benzylic amines using alkenes was investigated in detail, and the kinetic behavior of the direct C–H alkylation of benzylic amines using alkenes was studied. Kinetic evidence demonstrates that K_2CO_3 is only needed during an induction period to react with a Rh-species in solution to form the catalytically active species. In this induction period, K_2CO_3 is proposed to be dissolved to a vanishingly low extent into the reaction mixture and irreversibly reacts with a Rh-species to form a carbonato species. The duration of this induction period is dependent on the amount, the specific surface area and the H_2O content of K_2CO_3 and on agitation. It has to be tested whether the established kinetic description of the behavior of K_2CO_3 can also be applied to reactions in which it is a stoichiometric reagent rather than a cocatalyst. Additional experiments need to be performed to reveal the structure of the proposed catalytically active species and the nature of other Rh-species involved in the catalytic cycle.

4. EXPERIMENTAL SECTION

4.1. General Methods. In general, unless noted otherwise, chemicals were purchased from commercial suppliers and used without further purification. Compounds **1**¹⁷ and **1a**–**f**¹⁷ were synthesized according to literature procedures. Cyclooctadiene rhodium chloride dimer $[RhCl(cod)]_2$ was generally handled in a glovebox under argon. Dry and degassed toluene was purchased from commercial suppliers and stored over molecular sieves in a glovebox under argon. Water contents of K_2CO_3 batches were determined by measuring the loss on heating of the corresponding solids by heating a sample to about 200 °C under medium vacuum (0.1 mbar) overnight, assuming that only water was lost in the process. The same procedure was followed to obtain dry K_2CO_3 . Amounts of K_2CO_3 used in reactions were calculated assuming the solid to be completely dry, unless noted otherwise. Particle size distributions of K_2CO_3 batches were determined by laser diffraction using a dry powder dispersion unit for the sample introduction. Measurements were performed in 4-fold repetition, and the reported result is the average over all those four repetitions. Nitrogen adsorption and desorption experiments of K_2CO_3 batches were performed at 77 K. Sample size was chosen to provide at least 1 m² of total surface for the measurement. Degassing was performed at room temperature for 5 h directly before the adsorption and desorption measurements. Specific surface areas were determined from the obtained adsorption isotherms by the standard Brunauer–Emmett–Teller (BET) method. ¹H NMR spectra were recorded on a 400 MHz machine, and chemical shifts are reported in ppm, using Me_4Si as internal standard. GC measurements were carried out using a BGB-5 capillary column (30 m × 0.32 mm, 1.0 μm film, achiral) with the following oven temperature program: 100 °C (2 min), 18 °C·min⁻¹, 280 °C (5 min). GC yields were calculated by using the conversion factor of the corresponding compound relative to dodecane as internal standard, which was determined by calibration. Karl Fischer titrations were carried out using a stirring speed of 5. The corresponding water content values were calculated from the results of at least triplicate measurements.

4.2. General Procedure for Kinetic Experiments. All experiments were performed in oven-dried 8 mL vials with a fully covered solid Teflon-lined cap and a magnetic stirring bar, unless noted otherwise. Unless stated otherwise, the reaction mixtures were heated in a preheated aluminum reaction block (150 °C) and a stirring rate of 1400 rpm. Time measurement was started immediately after placing the vials in the aluminum block. Unless noted otherwise, quantifications were performed by means of GC analysis of the crude reaction mixtures using dodecane as internal standard and based on calibration curves for compounds **1**, **2**, **3**, and **4**, respectively, to determine their concentrations. Each kinetic experiment was performed in triplicate unless noted otherwise. GC measurements for quantifications were also performed in triplicate, the result for one sample was calculated as average over those three measurements, and the corresponding error was calculated as standard deviation over those experiments. Given values are therefore averages over three experiments, and the corresponding error is the standard deviation over those experiments. Unless noted otherwise, K_2CO_3 with an adsorbed water content of 15 mass %, a particle size median of 0.95 μm, and a specific BET surface of 0.8 m²·g⁻¹ was used. For every individual experiment, K_2CO_3 was placed in the vial. The vial was then transferred into a glovebox under argon. Cyclooctadiene rhodium chloride dimer (0.0313 mol·L⁻¹ solution), benzylic amine derivative (0.625 mol·L⁻¹ solution), and hex-1-ene (1.88 mol·L⁻¹ solution) were added in solutions inside the glovebox, and toluene as pure solvent was also added inside the glovebox. Reactions were stopped by immediately cooling them to room temperature in a water bath. Concentrations given for K_2CO_3 are not really concentrations because it is not completely dissolved in the reaction mixture. They can be viewed as molar loadings with respect to the total reaction volume. To estimate the total reaction volume, the volumes of all solutions and the pure solvent were assumed to be additive.

4.3. Initial Reaction Rates. The initial reaction rates are determined from two data points, the effective reaction start, and the yields of compounds **2** and **3** after a designated reaction time, which are determined in triplicate. The effective reaction start in initial rate experiments was determined to be 3.4 min.⁸ This effective reaction start compensates for the time the reaction mixture needs to reach a constant temperature. This value is used as the second data point for all initial rate experiments together with assumed product amounts of 0% to determine initial rates. Additionally, it should be noted that the formation of side product **4** was not observed to a detectable extent during the initial reaction period and was therefore not included in the initial rate calculation.

4.4. Induction Time Studies. Experiments were performed according to the general procedure for kinetic experiments. K_2CO_3 with an adsorbed water content of 2 mass %, a particle size median of 0.34 μm, and a specific BET surface of 0.4 m²·g⁻¹ was used. Dodecane was added as internal standard during the reaction. To take samples, the vial was opened inside a glovebox under argon after stopping the reaction. The vial was closed again, and the reaction was continued after taking each sample. Filtrations were performed using syringe filters with a pore size of 0.2 μm.

In the first experiment, $[RhCl(cod)]_2$, K_2CO_3 , hex-1-ene, and **1** with dodecane as internal standard were reacted for 10 min at 150 °C. After the reaction was stopped, the vial was transferred into a glovebox and the reaction mixture was filtered into another vial charged with a stirring bar. The solid residue in the first vial was washed two times with 0.5 mL of toluene before **1** (1 equiv) and hex-1-ene (3 equiv) with dodecane as internal standard were added. Both vials were heated again to 150 °C to restart the reaction. Additional samples of both reaction mixtures were taken.

In the second experiment, $[RhCl(cod)]_2$ and K_2CO_3 were reacted for 10 min at 150 °C. After the reaction was stopped, the vial was transferred into a glovebox. **1** (1 equiv), hex-1-ene (3 equiv), and dodecane as internal standard were added to the reaction mixture before filtration. The reaction mixture was filtered into another vial charged with a stirring bar. The vial containing the filtrate was heated again to 150 °C to restart the reaction. Additional samples of the reaction mixture were taken.

In the third experiment, $[\text{RhCl}(\text{cod})]_2$, K_2CO_3 and **1** with dodecane as internal standard were reacted for 10 min at 150 °C. After the reaction was stopped, the vial was transferred into a glovebox. Hex-1-ene (3 equiv) was added to the reaction mixture before filtration. The reaction mixture was filtered into another vial charged with a stirring bar. The vial containing the filtrate was heated again to 150 °C to restart the reaction. Additional samples of the reaction mixture were taken.

In the fourth experiment, $[\text{RhCl}(\text{cod})]_2$, K_2CO_3 and hex-1-ene were reacted for 10 min at 150 °C. After the reaction was stopped, the vial was transferred into a glovebox. **1** (1 equiv) and dodecane as internal standard were added to the reaction mixture before filtration. The reaction mixture was filtered into another vial charged with a stirring bar. The vial containing the filtrate was heated again to 150 °C to restart the reaction. Additional samples of the reaction mixture were taken.

4.5. Kinetic Time Course Comparison. Experiments were performed according to the general procedure for kinetic experiments. K_2CO_3 with an adsorbed water content of 2 mass %, a particle size median of 0.34 μm , and a specific BET surface of 0.4 m^2g^{-1} was used. Dodecane was added as internal standard during the reaction. To take samples, the vial was opened inside a glovebox after stopping the reaction. The vial was closed again, and the reaction was continued after taking each sample.

4.6. Electronic Influence on Benzylic Amines. All experiments were performed according to the general procedure for kinetic experiments. However, quantification of the reaction products was performed by ^1H NMR analysis of the crude residue in CDCl_3 after filtration of the reaction mixture and evaporation of the solvent with respect to DMSO as internal standard. In addition, for derivatives **1e** and **1f** ($\text{Y} = \text{CO}_2\text{Me}$ and CF_3 , respectively), the solubility in toluene was not high enough to prepare stock solutions with the same concentration as used for all other derivatives so these compounds were weighed directly as solids.

4.7. Temperature Dependence of the Initial Rate. All experiments were performed according to the general procedure for kinetic experiments. However, reaction mixtures were placed in a preheated oil bath at the desired temperature to control the temperature of the reaction mixture more precisely. In addition, reaction mixtures were only stirred moderately at a stirring rate of 375 rpm to provide for proper stirring inside the oil bath as well.

■ ASSOCIATED CONTENT

📄 Supporting Information

The Supporting Information is available free of charge on the ACS Publications website at DOI: 10.1021/acs.joc.5b01335.

Full experimental details, additional discussions, data points from kinetic experiments, and full mathematical details (PDF)

■ AUTHOR INFORMATION

Corresponding Author

*E-mail: michael.schnuerch@tuwien.ac.at

Notes

The authors declare no competing financial interest.

■ ACKNOWLEDGMENTS

We thank Professor Gerd Mauschwitz for help with particle size distribution measurements and Dr. Sven Barth and Dr. Jingxia Yang for help with nitrogen adsorption and desorption measurements.

■ REFERENCES

(1) (a) Zhang, M.; Zhang, Y.; Jie, X.; Zhao, H.; Li, G.; Su, W. *Org. Chem. Front.* **2014**, *1*, 843–895; (b) Schranck, J.; Thili, A.; Beller, M. *Angew. Chem., Int. Ed.* **2014**, *53*, 9426–9428; (c) Liu, B.; Shi, B. F.

Tetrahedron Lett. **2015**, *56*, 15–22; (d) Arnold, P. L.; McMullon, M. W.; Rieb, J.; Kühn, F. E. *Angew. Chem., Int. Ed.* **2015**, *54*, 82–100; (e) Shen, C.; Zhang, P.; Sun, Q.; Bai, S.; Hor, T. A.; Liu, X. *Chem. Soc. Rev.* **2015**, *44*, 291–314; (f) Musaev, D. G.; Figg, T. M.; Kaledin, A. L. *Chem. Soc. Rev.* **2014**, *43*, 5009–5031; (g) Djakovitch, L.; Felpin, F.-X. *ChemCatChem* **2014**, *6*, 2175–2187.

(2) (a) Hyster, T. K. *Catal. Lett.* **2015**, *145*, 458–467; (b) Ackermann, L. *Org. Process Res. Dev.* **2015**, *19*, 260–269; (c) Guo, T.; Huang, F.; Yu, L.; Yu, Z. *Tetrahedron Lett.* **2015**, *56*, 296–302; (d) Yuan, K.; Soulé, J.-F.; Doucet, H. *ACS Catal.* **2015**, *5*, 978–991; (e) Mo, J.; Wang, L.; Liu, Y.; Cui, X. *Synthesis* **2015**, *47*, 439–459; (f) Segawa, Y.; Maekawa, T.; Itami, K. *Angew. Chem., Int. Ed.* **2015**, *54*, 66–81; (g) He, R.; Huang, Z.-T.; Zheng, Q.-Y.; Wang, C. *Tetrahedron Lett.* **2014**, *55*, 5705–5713; (h) Yang, J. *Org. Biomol. Chem.* **2015**, *13*, 1930–1941; (i) Le Bras, J.; Muzart, J. *Synthesis* **2014**, *46*, 1555–1572.

(3) (a) Yan, G.; Borah, A. *J. Org. Chem. Front.* **2014**, *1*, 838–842; (b) Qiu, G.; Wu, J. *Org. Chem. Front.* **2015**, *2*, 169–178; (c) Dastbaravardeh, N.; Christakakou, M.; Haider, M.; Schnürch, M. *Synthesis* **2014**, *46*, 1421–1439; (d) Akhrem, I. S. *J. Organomet. Chem.* **2014**, *1–24*; (e) Weaver, J. F.; Hakanoglu, C.; Antony, A.; Asthagiri, A. *Chem. Soc. Rev.* **2014**, *43*, 7536–7547.

(4) (a) Wu, X.; Zhao, Y.; Zhang, G.; Ge, H. *Angew. Chem., Int. Ed.* **2014**, *53*, 3706–3710; (b) Petronilho, A.; Woods, J. A.; Mueller-Bunz, H.; Bernhard, S.; Albrecht, M. *Chem.—Eur. J.* **2014**, *20*, 15775–15784; (c) Xu, Y.; Zhou, J.; Zhang, C.; Chen, K.; Zhang, T.; Du, Z. *Tetrahedron Lett.* **2014**, *55*, 6432–6434; (d) Wei, Y.; Tang, H.; Cong, X.; Rao, B.; Wu, C.; Zeng, X. *Org. Lett.* **2014**, *16*, 2248–2251; (e) Fan, Z.; Song, S.; Li, W.; Geng, K.; Xu, Y.; Miao, Z.-H.; Zhang, A. *Org. Lett.* **2015**, *17*, 310–313; (f) Xu, H.; Muto, K.; Yamaguchi, J.; Zhao, C.; Itami, K.; Musaev, D. G. *J. Am. Chem. Soc.* **2014**, *136*, 14834–14844; (g) Yokota, A.; Aihara, Y.; Chatani, N. *J. Org. Chem.* **2014**, *79*, 11922–11932; (h) Ilangovan, A.; Satish, G. *Org. Lett.* **2013**, *15*, 5726–5729; (i) Li, B.; Bheeter, C. B.; Darcel, C.; Dixneuf, P. H. *Top. Catal.* **2014**, *57*, 833–842; (j) Loh, T.-P.; Wang, M.; Zhuang, Y.-X.; Xu, Y.-H.; Zhang, X. *J. Am. Chem. Soc.* **2015**, *137*, 1341–1347; (k) Kefalidis, C. E.; Davi, M.; Holstein, P. M.; Clot, E.; Baudoin, O. *J. Org. Chem.* **2014**, *79*, 11903–11910; (l) Kamal, A.; Srinivasulu, V.; Sathish, M.; Tangella, Y.; Nayak, V. L.; Rao, M. P. N.; Shankaraiah, N.; Nagesh, N. *Asian J. Org. Chem.* **2014**, *3*, 68–76; (m) Dang, Y.; Qu, S.; Nelson, J. W.; Pham, H. D.; Wang, Z.-X.; Wang, X. *J. Am. Chem. Soc.* **2015**, *137*, 2006–2014; (n) Roane, J.; Daugulis, O. *Org. Lett.* **2013**, *15*, 5842–5845; (o) Wang, X.; Wang, M. *Polym. Chem.* **2014**, *5*, 5784–5792; (p) Lian, Z.; Friis, S. D.; Skrydstrup, T. *Chem. Commun.* **2015**, *51*, 1870–1873.

(5) (a) Duan, P.; Lan, X.; Chen, Y.; Qian, S.-S.; Li, J. J.; Lu, L.; Lu, Y.; Chen, B.; Hong, M.; Zhao, J. *Chem. Commun.* **2014**, *50*, 12135–12138; (b) Sasaki, M.; Kondo, Y. *Org. Lett.* **2015**, *17*, 848–851; (c) Kommagalla, Y.; Mullapudi, V. B.; Francis, F.; Ramana, C. V. *Catal. Sci. Technol.* **2015**, *5*, 114–117; (d) Zhang, X.-S.; Li, Z.-W.; Shi, Z.-J. *Org. Chem. Front.* **2014**, *1*, 44–49; (e) Ricci, P.; Krämer, K.; Larrosa, I. *J. Am. Chem. Soc.* **2014**, *136*, 18082–18086. PMID: 25510851.

(6) (a) Mao, J.; Bao, W. *Chem. Commun.* **2014**, *50*, 15726–15729; (b) Aihara, Y.; Chatani, N. *J. Am. Chem. Soc.* **2014**, *136*, 898–901; (c) Chowdhury, S.; Chanda, T.; Koley, S.; Anand, N.; Singh, M. S. *Org. Lett.* **2014**, *16*, 5536–5539; (d) Chan, K. S.; Fu, H.; Yu, J.-Q. *J. Am. Chem. Soc.* **2015**, *137*, 2042–2046; (e) Bera, M.; Modak, A.; Patra, T.; Maji, A.; Maiti, D. *Org. Lett.* **2014**, *16*, 5760–5763; (f) Mercier, L. G.; Leclerc, M. *Acc. Chem. Res.* **2013**, *46*, 1597–1605; (g) Yang, T.; Zhang, T.; Yang, S.; Chen, S.; Li, X. *Org. Biomol. Chem.* **2014**, *12*, 4290–4294.

(7) (a) Dastbaravardeh, N.; Schnürch, M.; Mihovilovic, M. D. *Org. Lett.* **2012**, *14*, 3792–3795; (b) Dastbaravardeh, N.; Schnürch, M.; Mihovilovic, M. D. *Eur. J. Org. Chem.* **2013**, *14*, 2878–2890.

(8) Pollice, R.; Dastbaravardeh, N.; Marquise, N.; Mihovilovic, M. D.; Schnürch, M. *ACS Catal.* **2015**, *5*, 587–595.

(9) In fact, every catalytic reaction consisting of at least two consecutive steps has an induction period. However, if the induction period is very short, it is usually stated that there is none which actually means that it is negligible.

(10) (a) Jia, W.-G.; Han, Y.-F.; Jin, G.-X. *Organometallics* **2008**, *27*, 6035–6038; (b) Ellul, C. E.; Saker, O.; Mahon, M. F.; Apperley, D. C.; Whittlesey, M. K. *Organometallics* **2008**, *27*, 100–108; (c) Guo, J.; Lv, L.; Wang, X.; Cao, C.; Pang, G.; Shi, Y. *Inorg. Chem. Commun.* **2013**, *31*, 74–78.

(11) The reaction was not even finished after 24 h.

(12) Due to simplifications in the derivation this equation is only valid when the amount of K_2CO_3 that is dissolved and bound is negligible to the total amount.

(13) Yang, H.-M.; Wu, P.-I. *Appl. Catal., A* **2001**, *209*, 17–26.

(14) Hammett, L. P. *J. Am. Chem. Soc.* **1937**, *59*, 96–103.

(15) Because the initial rates were determined by 1H NMR analysis the formation of byproduct **3** could not be reliably quantified and was therefore neglected.

(16) Eyring, H. *J. Chem. Phys.* **1935**, *3*, 107–115.

(17) Dastbaravardeh, N.; Kirchner, K.; Schnürch, M.; Mihovilovic, M. *J. Org. Chem.* **2013**, *78*, 658–672.